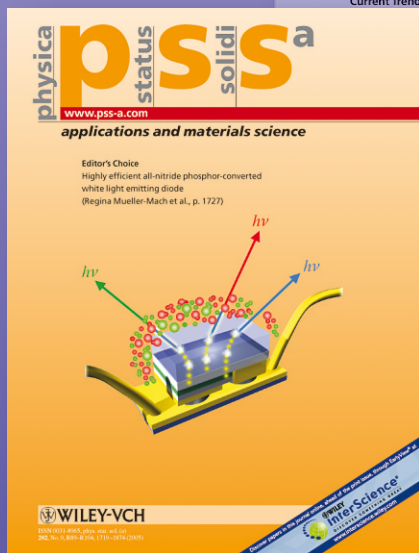


physica **p** status **s** solidi **s**

www.interscience.wiley.com

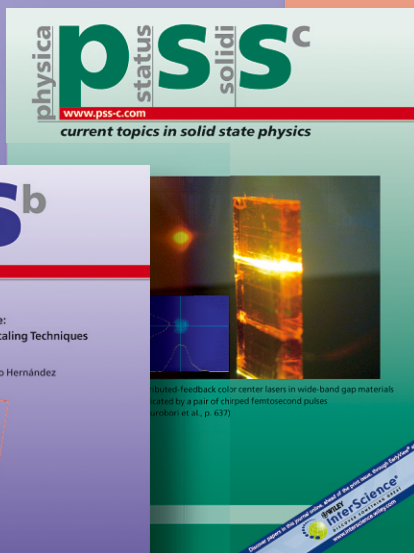
reprints



www.pss-a.com



www.pss-b.com



www.pss-c.com



www.pss-rrl.com

Sintering of yttria-stabilized zirconia nanopowders studied by positron annihilation spectroscopy

J. Čížek¹, O. Melikhova¹, J. Kuriplach¹, I. Procházka^{*,1}, T. E. Konstantinova², and I. A. Danilenko²

¹ Charles University in Prague, Faculty of Mathematics and Physics, Department of Low Temperature Physics, V Holešovičkách 2, 180 00 Praha 8, Czech Republic

² Galkin Donetsk Institute for Physics and Engineering, National Academy of Science of Ukraine, Luxemburg Street 72, 831 14 Donetsk, Ukraine

Received 15 January 2009, accepted 1 June 2009

Published online 7 October 2009

PACS 61.46.Hk, 61.72.J-, 78.70.Bj, 81.07.Wx, 81.40.Ef

* Corresponding author: e-mail: ivan.prochazka@mff.cuni.cz, Phone: +420-2-21912769, Fax: +420-2-21912567

A positron annihilation study of the tetragonal yttria-stabilized zirconia (YSZ) nanopowder compacted under a high pressure and subjected to a sintering at temperatures ranging from 1000 to 1350 °C were investigated. The conventional positron lifetime and coincidence Doppler broadening measurements were performed. In the compacted nanopowder, positrons were found to annihilate mainly as trapped at vacancy-like de-

fects (most likely the Zr vacancies) situated in the negative space-charge layers along grain boundaries (GB's) or at larger defects associated with GB intersections (triple points). Moreover, pores of a few-nanometer size were detected via positronium pick-off annihilation in the YSZ nanopowders. These pores, however, disappeared after sintering at 1000 °C and a significant grain growth takes place above this temperature.

© 2009 WILEY-VCH Verlag GmbH & Co. KGaA, Weinheim

1 Introduction Zirconia (ZrO_2) is a base ingredient of many industrially attractive materials, especially when high-temperature applications are required (the melting point of ZrO_2 is 2700 °C). The advantageous properties can be enhanced in the *nanostructured* zirconia-based materials. However, the use of the *pure* zirconia is limited because of a transition from a room-temperature monoclinic to a more dense tetragonal phase at ≈ 1100 °C. Such a phase transition is accompanied with a large volume shrinkage and, consequently, cracks within material structure may appear. A stabilization of the high-temperature tetragonal phase can be reached by an addition of a certain amount of Y_2O_3 (yttria) to form a solid solution with zirconia [1]. Such a kind of systems is referred to as yttria-stabilized zirconia (YSZ). The tetragonal YSZ system is formed with ≈ 3 mol.% of yttria [1].

A solution of the yttria in zirconia leads to a violation of the stoichiometry resulting in a formation of a huge amount of vacancies (mainly the oxygen vacancies) and

vacancy–solute atom complexes in the ZrO_2 lattice. In the nanostructured YSZ materials, the defects associated to grain boundaries (GB's), i.e. vacancy-like defects, triple points, voids and pores may occur in addition. These open-volume structures can in turn influence macroscopic properties. Consequently, a detailed knowledge of defect nature and behavior, especially at elevated temperatures, is of a crucial importance, e.g. for a controlled prospecting of YSZ materials for technological applications.

Obviously, open-volume structures in YSZ nanomaterials are a challenge for positron annihilation spectroscopy (PAS) Although several earlier papers treated this topic [2–6], there is still a lot of missing information, for example, on the nature of point defects and details of microstructure evolution in the YSZ nanopowders subjected to a sintering process.

Recently, we have employed the positron lifetime (LT) and the coincidence Doppler broadening (CDB) techniques in investigations of the compacted YSZ nanopowders [7,

8]. Extensive theoretical calculations of positron parameters in YSZ lattice have been performed by us, too [9, 10]. A potential use of the short-lived LT components for disclosing further details of sintering process in the YSZ nanopowders was discussed in Ref. [8]. In the present Contribution, therefore, we focus on the microstructural changes induced in the tetragonal $\text{ZrO}_2+3 \text{ mol.}\% \text{ Y}_2\text{O}_3$ during sintering nanopowders.

2 Experimental

2.1 Samples

The initial nanosized $\text{ZrO}_2+3 \text{ mol.}\% \text{ Y}_2\text{O}_3$ powder was prepared by the coprecipitation technique which was presented in details elsewhere [11, 12]. After a calcination at a temperature of 700 °C for 2 hours, the nanopowder was uniaxially pressed under 500 MPa to form tablets of ≈ 5 mm thickness and ≈ 10 mm diameter. The tetragonal phase and an average size of nanopowder particles were determined by means of TEM or XRD for the initial powder (17 nm) as well as for specimens after sintering.

The compacted $\text{ZrO}_2+3 \text{ mol.}\% \text{ Y}_2\text{O}_3$ tablets were subjected to sintering at three different temperatures, $T_S = 1000, 1200$ and 1350 °C, in air for 2 hours. Potential effects of a preliminary compression of initial powder was also examined by pressing some specimens under 200 MPa prior to granulation. Before the measurements were started, each specimen had been dried at 105 °C in air for 1 hour.

The positron source was made of about 1.3 MBq of carrier-free ^{22}Na (iThemba Labs) sealed between the 4 μm thick mylarC foils (DuPont). The source was sandwiched with the identical tablets of the material studied.

2.2 Apparatus and data acquisition The LT measurements were performed using a BaF_2 spectrometer [13] operated in the fast-fast configuration. Using the above positron source–specimen sandwich, the spectrometer exhibited a time resolution of 160 ps (FWHM for ^{22}Na) and $\approx 80 \text{ s}^{-1}$ coincidence count rate. Approximately 10^7 coincidence events were accumulated in each LT spectrum. A maximum-likelihood procedure [13] was utilized to decompose the LT spectra into discrete components. The annihilation of positrons in the source salt and covering foils was determined from separate LT spectra measurements with a well-annealed α -iron reference specimen.

The CDB experiments were carried out using a two-detector (HPGe) coincidence spectrometer [14] showing an energy resolution of 1.1 keV (FWHM) at the 511 keV energy, a coincidence count rate of $\approx 500 \text{ s}^{-1}$ and a peak-to-background ratio of $\approx 10^5$. At least 10^8 counts were collected in each two-dimensional CDB spectrum. The results of the CDB measurements are expressed as the Doppler-broadened profiles (DBP) related to the DBP of a well-annealed pure Zr reference specimen.

3 Results and discussion

3.1 LT measurements The lifetimes and relative intensities resulting from the decomposition of the measured LT spectra into individual components are collected in Table 1. The two components were observed in samples sintered at $T_S = 1000$ and 1200 °C. Obviously, a preliminary pressure treatment of the samples had no influence on the observed LT parameters. Average lifetimes $\tau_{\text{av}} = \sum_i \tau_i I_i$ were included in the table, too. A remarkable decrease of τ_{av} with sintering temperature evidences that a recovery of open-volume defects takes place during sintering. By similarity of present lifetimes with those observed for compacted $\text{ZrO}_2+3 \text{ mol.}\% \text{ Y}_2\text{O}_3$ and other similar YSZ nanopowders at the room temperature [7, 8] we attribute τ_2 - and τ_3 -components of Table 1 to the annihilation of positrons trapped in vacancy-like defects situated in the space charge layers along the GB's ($\tau_2 \approx 0.180$ ns) and triple points ($\tau_3 \approx 0.375$ ns). Based on simple spatial considerations, the intensity ratio I_3/I_2 was found to correlate with average grain size d as $I_3/I_2 \sim d^{-2}$. A pronounced decrease of I_3/I_2 with increasing T_S thus indicates that a remarkable grain growth takes place during sintering. Thus, the τ_2 -component in the specimen sintered at 1200 °C is expected to contain also a contribution from positron trapped in defects inside grains known from the investigations on YSZ single crystals [6, 8].

A different pattern of LT spectrum was, however, exhibited by the specimen sintered at $T_S = 1350$ °C. The τ_3 -component (triple points) completely vanishes. A mean grain size of ≈ 250 nm was indicated by XRD for this case and positron annihilation in the grain interiors dominates. In addition, a weak short-lived component corresponding obviously to the annihilation of delocalized positrons was resolved in LT spectrum.

Contrary to the case of non-sintered compacted YSZ nanopowders, in which ortho-Ps components with pick-off lifetimes of $\tau_{\text{O-Ps}} \approx 30$ ns and $I_{\text{O-Ps}} \approx 7\%$ were observed [7], no Ps formation was detected in specimens subjected to sintering. This is in accordance with the earlier paper [3] in which a disappearance of pores in sintered commercial $\text{ZrO}_2+2 \text{ mol.}\% \text{ Y}_2\text{O}_3$ nanopowders was observed at the sintering temperatures ranging from 800 to 1200 °C.

3.2 CDB results The observed DBP ratios for $T_S = 1000$ and 1200 °C are shown in Fig. 1 together with the DBP's for the virgin compacted nanopowders and the tetragonal YSZ single crystal taken for a comparison. With increasing T_S , an approaching of the DBP ratios to that obtained for the $\text{ZrO}_2+3 \text{ mol.}\% \text{ Y}_2\text{O}_3$ single crystal is seen from the figure. This result can be understood as a consequence of increasing grain size during sintering leading to a decrease of a fraction of positrons annihilating in the negative space-charge layers along GB's. In the low-momentum region, DBP ratios for sintered specimens are suppressed compared to the virgin compacted $\text{ZrO}_2+3 \text{ mol.}\% \text{ Y}_2\text{O}_3$ nanopowder. Such a decrease is obviously connected with a decreasing open-volume defect

Table 1 Positron lifetimes τ_i and relative intensities I_i obtained for the sintered $\text{ZrO}_2+3 \text{ mol.}\% \text{ Y}_2\text{O}_3$ nanopowders. Relative intensities were normalized so that $\sum_i I_i = 100 \%$. The ortho-positronium (Ps) components were observed in non-sintered nanopowder, too [7, 8], but they were omitted in the table. Errors (1 std deviations) are given in the units of the last significant digit.

T_S [°C]	Pre-presurized	τ_1 [ns]	I_1 [%]	τ_2 [ns]	I_2 [%]	τ_3 [ns]	I_3 [%]	τ_{av} [ns]
^{a)}	no			0.186(3)	33(1)	0.383(2)	67(1)	0.318
	yes			0.190(4)	33(1)	0.381(4)	67(1)	0.318
1000	no			0.185(2)	77(1)	0.374(2)	23(1)	0.228
	yes			0.188(2)	80(1)	0.374(2)	20(1)	0.225
1200	no			0.185(1)	99(1)	~0.374	1(1)	0.187
	yes			0.185(1)	98(1)	~0.374	2(1)	0.189
1350	no	0.035(9)	7(1)	0.178(1)	93(1)			0.168
	yes	0.040(9)	7(1)	0.179(1)	93(1)			0.169

^{a)} The initial nanopowder.

concentration (mainly triple points) during sintering and also with the absence of Ps formation in the sintered specimens. The amplitude of a peak at $p \approx 15 \times 10^{-3} m_0c$, which is known to origin from the positron annihilation with the oxygen electrons, is increased with rising T_S . This finding again reflects an increasing fraction of positrons annihilating inside grains.

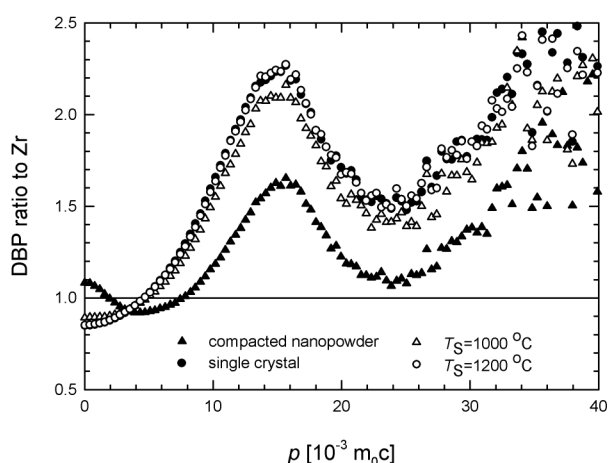


Figure 1 DBP ratios for $\text{ZrO}_2+3 \text{ mol.}\% \text{ Y}_2\text{O}_3$ nanopowders sintered at various temperatures T_S , including starting compacted nanopowder, and for $\text{ZrO}_2+3 \text{ mol.}\% \text{ Y}_2\text{O}_3$ single crystal.

4 Summary A significant grain growth was observed in the pressure-compacted $\text{ZrO}_2+3 \text{ mol.}\% \text{ Y}_2\text{O}_3$ nanopowders sintered at $T_S = 1000$ and 1200 °C and, moreover, a more detailed data on the defect behavior could be obtained. The PAS techniques (LT and CDB) were thus demonstrated to be capable of observing the sintering process even in the conditions when no Ps formation occurs.

Acknowledgements The present work was supported by The Ministry of Education, Youths and Sports of the Czech Republic – the scientific plan No. 0021620834, The Czech Scientific Foundation – contract No. GA 106/06/0270, and The Grant Agency of the Academy of Sciences of the CR – projects Nos. KAN300100801 and KJB101120906. The financial support from The National Academy of Science of Ukraine (scient. plans Nos. A 116/06 H and A 106U006933) is also acknowledged.

References

- [1] See, e.g., <http://www.stanfordmaterials.com>.
- [2] K. Ito, H. Nakanishi, and Y. Ujihira, *J. Phys. Chem. B* **103**, 4555 (1999).
- [3] Y. Yagi, S. Hirano, Y. Ujihira, and M. Miyayama, *J. Mater. Sci. Lett.* **18**, 205 (1999).
- [4] J. E. Garay, S. C. Glade, P. Asoka-Kumar, U. Anselmi-Tamburini, and Z. A. Munir, *Journ. Appl. Phys.* **99**, 024313 (2006).
- [5] R. I. Grynszpan, S. Saude, L. Mazerolles, G. Brauer, and W. Anwand, *Radiat. Phys. Chem.* **76**, 333 (2007).
- [6] J. Cizek, O. Melikhova, J. Kuriplach, I. Prochazka, T. E. Konstantinova, and I. A. Danilenko, *Phys. Status Solidi C* **4**, 3847 (2007).
- [7] I. Prochazka, J. Cizek, J. Kuriplach, O. Melikhova, T. E. Konstantinova, and I. A. Danilenko, *Acta Phys. Polon. A* **113**, 1495 (2008).
- [8] O. Melikhova, J. Kuriplach, J. Cizek, I. Prochazka, W. Anwand, G. Brauer, T. E. Konstantinova, and I. A. Danilenko, *Phys. Status Solidi C* **4**, 3831 (2007).
- [9] O. Melikhova, J. Kuriplach, J. Cizek, I. Prochazka, and G. Brauer, *Mater. Sci. Forum* **607**, 125 (2009).
- [10] A. M. Slipenyuk, M. D. Glinchuk, I. P. Bykov, A. V. Ragulya, V. P. Klimenko, T. E. Konstantinova, and I. A. Danilenko, *Ferroelectrics* **298**, 289 (2004).
- [11] T. Konstantinova, I. Danilenko, N. Pilipenko, and A. Dobrikov, 9th Cimtec – World Ceramic Congress. *Ceramics: Getting into the 2000's – Part A*, (Techna Group s.r.l., Faenza, Italy, 2004), p. 305.
- [12] F. Becvar, J. Cizek, L. Lestak, I. Novotny, I. Prochazka, and F. Sebesta, *Nucl. Instrum. Methods Phys. Research A* **443**, 557 (2000).
- [13] J. Cizek, F. Becvar, I. Prochazka, and J. Kocik, *Mater. Sci. Forum* **445-446**, 63 (2004).